THE ARCHIVE OF MECHANICAL ENGINEERING

Vol. LI 2004 Number 2

Key words: *identification, vibrations, beams, Dynamic Stiffness Matrix*

*STANISŁAW A. LUKASIEWICZ**), *EMILY R. QIAN**)

APPLICATION OF THE DYNAMIC STIFFNESS MATRIX TO THE IDENTIFICATION OF CRACKS IN BEAMS AND FRAMES

The paper discusses the problem of the accuracy of the identification techniques detecting cracks and corroded members in vibrating beam and frame structures. The presence of the fatigue crack usually causes very small changes of the stiffness of the beam elements of the structure. To detect these changes it is necessary to apply the most precisely mathematical detection technique. The identification procedure based on the least squares technique uses finite element models (FEM) of the structure and as the source of information the measured dynamic response and the natural frequencies. The application of the Dynamic Stiffness Matrix (DSM) [1] for the representation of all constraints and modal equations makes it possible to present the identification process in a very accurate and efficient mathematical form. The methoyof d of the detection of structural changes used in the present paper was described in our previous paper [2]. The Consistent Mass Matrices (CMM) and Lump Mass Matrices (LMM) are very often used in the identification algorithms. It is shown that application of simplified approaches (CMM and LMM) can result in lower accuracy and poorer convergence of the identification algorithms. However, the application of CMM mass matrices does not introduce significant errors. The algorithms were tested on simulated numerical data for ten element beam frames.

1. Introduction

Defects, such as cracks or corrosion, change the local stiffness of the elements of the vibrating structure, which results in the change of the dynamic behaviour of the whole structure. Propagation of cracks and other failures of the members produce changes in the bending and axial stiffness of the members. Observing the change in the bending stiffness caused by the closing

*) *Departament of Mechanical Engineering The University of Calgary, Calgary Alberta, Canada; E-mail: lukasiew@ucalgary.ca*

and opening of the crack in two different configurations makes it possible to detect the crack. Corrosion reduces the stiffness of the member, and the change does not depend on the deformations of the member during its motion. In contrast, a crack changes the stiffness of the element only when it is open. When the crack is closed the changes introduced by the closed crack are small enough to assume that there is no significant change in the stiffness of the element. This observation can be used to differentiate cracks from corrosion. The first analysis of the behavior of a beam with cracks was done fifty years ago in the USA. In 1944 P.G. Kirmser [16] discussed the effect of the crack on the natural frequencies of a vibrating beam. Later W.T. Thomson [34] investigated the possibility of detecting cracks in slender bars. Although he only attempted to determine theoretically the effect of flexible discontinuities on flexural, longitudinal, and torsional vibration of slender bars, he expressed his belief in the possibility to determine the position and depth of a crack by carrying out experiments. Using ideas from Kirmser's research, he approached the problem using the operational method based on Laplace transformation. He was able to determine the influence of a slot on the natural frequency of a beam and found that for very small cracks the influence on the natural frequency is negligible. However, for deeper slots the changes increase quite rapidly. In 1981 H.J. Petroski [28], using the same approach as M. Hetenyi [11], P. Kirmser [16] and W.T Thomson [34], represented the deflection of a beam in his analysis using Fourier series. He related Stress Intensity Factor K to the deflection of a beam for static and dynamic cases. He demonstrated that the crack increases the overall vibration amplitude of the beam.

Interest in the problem of cracked beams has increased in recent years since failure analysis and prediction have become an issue in engineering practice. Researchers have become interested in the problems related to eigenfrequency changes in structures due to cracks. R.D. Adams and P. Cawley [1] used a method based on sensitivity analysis to deduce the location of damage and the FEM to represent the model of the structure. A year later, in 1984, M.M.F. Yuen [34] presented results from his research in which he wanted to find the relationship between damage location, damage size and the changes in the eigenvalues and eigenvectors of a cantilever beam subjected to damage. See also papers [3], [7], [8] devoted to similar problems.

In 1990, G.-L. Qian, S.-N. Gu and J.-S. Jiang [28] published the results of the investigation of the dynamic behavior and crack detection of a beam with a crack. Calculated values were compared with the experimental data

obtained from the work of P. Gudmundson. The article presented by P.F. Rizos, N. Aspragathos and A.D. Dimarogonas [31] on identification of crack location and magnitude in a cantilever beam, as all previously presented methods, neglects damping. A different method, utilizing the relation between the changes in the eigenfrequencies, the local stiffness losses and the mode shape functions of the undamaged system, was presented in 1993 by U. Pabst and P. Hagedorn [25]. Rayleigh's Quotient was used as a base for the crack detection procedure. Being aware of the limitations of the previously presented methods, A. Morassi [23] used a perturbation method to evaluate the first order perturbation of the eigenfrequencies. Two years later, in 1995, W.M. Hasan [9] extended the above work to the case of a beam on an elastic foundation and was able to find the position and severity of a crack using the same approach as A. Morassi. See also papers [2], [13], [14].

The ability to locate and assess damage in flexible truss structures has progressed considerably in the last five years. Many local (measurement) approaches have been developed and evaluated previously, including X-ray, optical, infrared, and ultrasonic methods. Global methods (mathematical approaches), currently under development, use vibration response and system identification techniques to detect damage in flexible structures. Almost all approaches are based on eigenvalue and eigenvector derivatives. S.L. Hendriks et al. [10] presented an eigenvalue sensitivity identification procedure and performed a numerical simulation to obtain clustered and lowfrequency vibration modes, characteristic of large flexible structures. Mass, damping and stiffness matrices were constructed in terms of small sets of physical property parameters. Estimation and correction of initial parameters was accomplished by using firstorder eigenvalue derivatives and the difference between the measured and predicted frequencies. Using the eigenvalue sensitivity method, less information about the system is needed than using the eigenvector sensitivity method. The second method is expected to be more efficient. C. Flanigan [5] applied an eigenvector sensitivity approach for model refinement of a truss structure. The illustration of this method was presented by J.M. Ricles and J.B. Kosmatka [30]. First, residual modal force vectors were used to locate the damage. Second, a weighted eigenvector sensitivity analysis was carried out to estimate the extent of the damage. S.W. Smith and C.A. Beattie [33] incorporated the incomplete measurement procedure for damage assessment but not for damage location.

An advantage of sensitivity identification is that the damage can be assessed with incomplete measurements. Also, areas in a property matrix far from damaged areas remain unaffected by using a localized set of physical parameters. A disadvantage is that an inclusive set of physical parameters

must be defined before sensitivity analysis can be successful. Experiments show that algorithms are often not robust with respect to errors in the modal data, and lead to numerical difficulties with near-singular sets of equations. R.M. Lin [17] proposed an improved method that employs analytical and experimental data, both eigenvalues and eigenvectors, to calculate sensitivity coefficients. Numerical experiments with a truss structure indicate that this method overcomes difficulties associated with previous procedures, such as slow convergence and ability to handle small damage. See also [14], [22].

Multiple-constraints matrix adjustment identification methods have shown promise in determining damage location and assessment in flexible structures. S.W. Smith and S.L. Hendrix [32] presented a detailed review of these methods. Through the solution of the constrained optimization problem, formulated with the matrix Forbenious norm, this approach produces adjusted FEM property matrices that more closely match the structural properties determined from tests of the structure. Stiffness loss in the FEM model is established to determine damage severity and location.

For better detection of damage in a flexible structure, the hybrid approach that combined the advantages of both eigensensitivity and matrix adjustment techniques, was investigated by Cuiping Li and Smith S.W. [4]. The first multiple-constraint stiffness matrix adjustment algorithms were used to formulate the general form of the objective function to minimize the Frobenius norm of the matrix of residual force vectors. Only an undamped system was considered. Later physical parameter sensitivities were introduced through a first-order expansion of the stiffness matrix. As a result, the least square problem was solved to identify the set of physical property parameters. From acceleration data obtained corresponding to all DOF, eigenfrequencies and modal shapes were computed as input data for system identification. An experiment conducted with a truss structure with 96 DOF confirms the ability of the method to identify the damage location.

The experimental measurement of the dynamic system is usually pursued through determination of the natural frequencies and modes of a structure and comparison with the analytical system response data. Many test procedures have been proposed [12] to determine eigenfrequencies and modal shapes of a structure from experimental measurements.

They vary in the manner in which the structure is excited, the quantities, which are measured, and the manner in which the experimental data are analyzed. Most modal vibration methods are based on the assumption that there is no mode coupling. Although some methods have been introduced to deal with modal interference, they require advanced determination that mode coupling will occur and their accuracy is not much better than that of other

methods. However, to obtain modal data one is not required to measure the response of the structure at all nodal degrees of freedom. The aforementioned methods received the most attention in the past. The direct use of dynamic response measurements from all degrees of freedom was also examined. This approach allows determining the modal characteristics of a structure more accurately. Also some different methods were applied to identify the dynamic system [8]. Statistical parameter estimation [13], [18], matrix perturbation theory [5], the matrix adjustment procedure [15], simultaneous expansion and orthogonalization of measured modes [33] or hybrid approach [4], [35] are just a few methods presented in the past. There is no obvious choice since all of them have some limitations. The monograph by M.I. Friswell and Mottershead [6] published in 1995 describes different methods for identification and model updating. However, the approach and the formulation applied in the present paper are not presented there.

As mentioned before a simple and straightforward but very efficient approach was presented in [19], [20], [21]. This method is based on the least square technique and minimization of the global error functional. Using directly measured data from all nodal degrees of freedom the dynamic system was identified. It was also shown that due to the matrix formalization of all operations the method was able to deal with noisy data and provide very accurate results. This method is used in the present paper to detect the defects in beams and trusses (see also [26], [37] for details).

In recent years, considerable effort has been devoted to investigation of the relationship between crack location, crack size and the corresponding changes in modal shapes and eigenfrequencies. The studies in this area have been mostly limited to beam elements with local cracks. There has been less research done to establish an effective, general method to analyse more complex structures, such as trusses and to detect damage from monitoring of vibration. Also, the previous works used changes in natural frequencies and/or modal shapes of locally damaged structures.

The get high precision of the results necessary in the identification process it is suggested to use a dynamic stiffness matrix (DSM) in which the stiffness matrix of the structure is assembled directly from the differential equations of motion and thus internal effects of the vibrating masses. In this way there is no mass matrix involved. The shape functions that are used for derivation of the stiffness matrix are exact solutions of the differential equation of motion. Thus the calculated eigenvalues and natural frequencies are exact. Classical approach in FEM is based on the assumption that the local behaviour within the element determines the stiffness and mass matrices of the structure. The accuracy of the results strongly depends on the accuracy of the element

modelling. In the case of the static analysis of the frames the FEM solution is correct. However, the exact dynamic description of the system is necessary for the purpose of the identification.

The identification algorithm proposed here using DSM generates very precise results which allow to identify even small changes in the bending stiffness of the members resulting from cracks and corrosion. The method was tested on simulated experimental data. The results obtained from DSM approach were compared to the results obtained using CMM and LMM. When the displacements or accelerations at all degrees of freedom are used as measured data the calculations converge rapidly to the correct solution. The method is working also on the incomplete set of data.

2. Identification technique

To show that the changes of the stiffness are small we present here the results of the calculation of the change of the stiffness of the beam

Throughout the formulation and evaluation process, it has been assumed that:

(1) Accelerations and displacements are the measured quantities representing dynamic response of a structure.
(2) The only changes associated with occurrence of cracked and corroded members are changes in stiffness of a structure. Therefore, changes in mass or damping properties are not considered.
(3) The structure vibrates freely during the period of time of the analysis.

2.1 Stiffness changes in structures due to cracks and corrosion

The loss of the axial or bending stiffness of a beam due to a transverse crack can be examined using FEM. [1]. The equivalent flexural rigidity EI_z for the cracked member with dimensions $h \times 1 \times L$ can be represented φ as:

$$\frac{EI_z}{EI_o} = \frac{1}{1 - \frac{10h}{L}\left(1 - \frac{1}{k_e}\right)} \tag{1}$$

where k_e is a stiffness reduction coefficient presented in Figure 1. EI_o is the stiffness of the sections without a crack. Fig. 1 and Eq. (1) can be used to find the crack length in the analysed member if the actual stiffness is known.

We see that the crack initially changes very little the stiffness of the beam. Crack of the depth of 10% thickness of the beam results in 2% change of the

flexural stiffness of the beam only. It is therefore of extreme importance to be able to detect the stiffness changes with as high precision as possible. It is assumed in the paper that the crack changes the stiffness of the member only when it is opened. That relates the crack to the sign of the deflection curvature. The corrosion changes the stiffness of a member irrespective of the beam curvature.

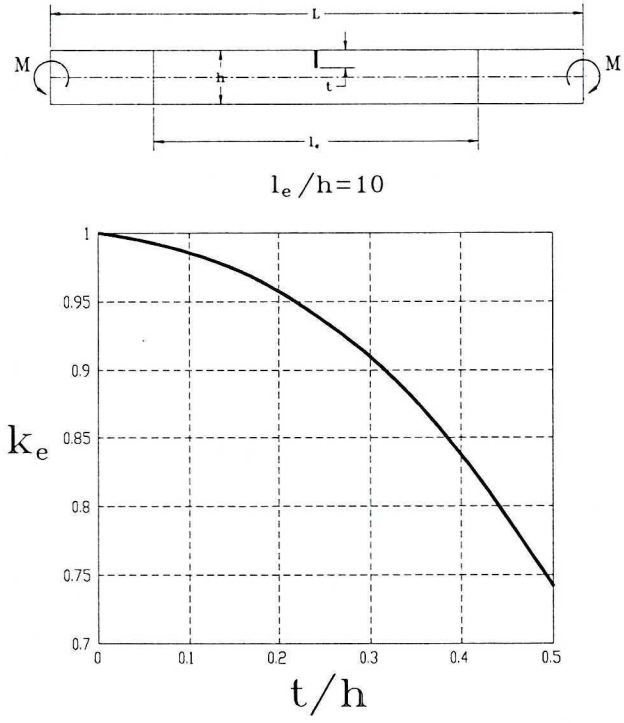

Fig. 1. Stiffness reduction coefficient for the cracked beam, t is the crack depth

Dynamic behaviour of structures depends on a number of properties. These properties, such as mass, stiffness and damping characteristics of members can be significantly affected by changes in the structure due to corrosion or cracks. When dealing with changes caused by corrosion, the effect of the cross-section area decrease is simply predictable. A smaller crosssection area gives smaller flexural and axial stiffness of the element. Also the mass of the affected element decreases. However, this change can be related to the change of the bending stiffness parameter.

Damping properties are also likely to be affected, but their actual influence is not exactly known, and only experimental work can provide an answer to this problem. Since for the loaded structure, the effect of stiffness and mass changes are most significant, damping changes of the beam element are not taken into consideration in this study.

When cracks appear in vibrating structures, their influence on the behaviour of the structure is more complex. The loss of stiffness only occurs for the Open Crack Mode. It is assumed that in the Closed Crack Mode there are no stiffness changes of the element. This is an accurate enough approximation of the real behaviour of very fine cracks since stress changes induced by contact of closed surfaces of a crack are very local and relatively small. The stiffness of the element can only decrease due to crack appearance. The curvature of the member can be established by knowing the angular displacement of the member at both ends. This procedure is only appropriate if the element is vibrating in its first mode. If the structure is excited in a controllable way, this requirement can be simply satisfied. If not, the structure must be divided into more elements to satisfy the condition that each member is in the first mode of vibration.

The influence of artificially generated measurement error on the accuracy of the solution was investigated. The model system equations are considered as constraint equations for an optimisation problem where the differences between the measured values and the values predicted by the model are minimised.

2.2 Method

A general dynamic system modelled using the finite element method is presented by a matrix equation

$$K(\omega)u - F \tag{2}$$

where K is the global dynamic stiffness matrix and F is the vector of external forces. In this case F is equal to zero since only free vibration is considered. The matrix K has dimensions n × n, where n is the number of degrees of freedom of the system. Let us assume that displacement u^* or acceleration vector a^* is measured and m values for each n DOF are obtained. Two vectors of accelerations a_{nm} and a^*_{mn} are created. The vectors predicted by the model:

$$\begin{aligned} u^T &= [u_{11}, u_{12} \ldots u_{1m}, u_{21}, u_{22} \ldots u_{2m}, \ldots, u_{n1} \ldots u_{nm}]^T \\ a^T &= [a_{11}, a_{12} \ldots a_{1m}, a_{21}, a_{22} \ldots a_{2m}, \ldots, a_{n1} \ldots a_{nm}]^T, \end{aligned} \tag{3}$$

The vectors of measured displacements or accelerations are:

$$\begin{aligned} u^{*T} &= [u^*_{11}, u^*_{12} \ldots u^*_{1m}, u^*_{21}, u^*_{22} \ldots u^*_{2m}, \ldots, u^*_{n1} \ldots u^*_{nm}]^T \\ a^{*T} &= [a^*_{11}, a^*_{12} \ldots a^*_{1m}, a^*_{21}, a^*_{22} \ldots a^*_{2m}, \ldots, a^*_{n1} \ldots a^*_{nm}]^T, \end{aligned} \tag{4}$$

where m is the number of samples for each displacement or acceleration a_n.

The values of u^* and a^* are affected by noise and other experimental errors. The matrix K is also unknown and should be found from the analysis of the experimental data. To find u, and K, the method of least squares has been applied. Let us define the global error of measurements R, in the time interval T, as follows:

$$R = \frac{1}{2}(u - u^*)^T (u - u^*) + \frac{1}{2} W_1(\omega - \omega^*) + \lambda(K(\omega)u - F) + W_2\lambda_1 D(\omega), \quad (5)$$

where λ is the vector of the Lagrangian multipliers,

$$[\lambda]^T = [\lambda_{12}, \lambda_{13} \ldots \lambda_{1,m-1}, \lambda_{22}, \lambda_{23} \ldots \lambda_{2,m-1}, \ldots, \lambda_{n2} \ldots \lambda_{n,m-1}]^T, \quad (6)$$

and ω, ω^* are calculated and measured natural frequencies of the system. W_1 and W_2 are the weights for the data for ω and ω^*.
Equation $D(\omega) = |K(\omega)| = 0$. represents here the eigenvalue equation used to calculate the natural frequencies of the vibrating system. This equation is often difficult to solve precisely due to numerical problems in the calculations involving the trigonometric functions. In the presented approach this equation is not solved directly to obtain the values of ω_i. It is only checked in the iterations and the values of the natural frequencies are obtained as the result of the optimization process. Due to the effect of the defects in elements the matrix K, changes, these changes, however, can be defined by the changes of parameters p_i which are related to the properties of the elements of the system.

The stiffness matrix K^e of an element i can be presented in the form:

$$K^e{}_i = p_i k_i, \quad (7)$$

where p_i is a scalar coefficient characterising the physical properties of the element i and k_i is the normalised stiffness matrix of the element i. This means that the properties of the element are characterised by one parameter only. This is justified when we can neglect the bending stiffness as compared to the axial stiffness while analysing trusses, or the axial stiffness as compared to the bending stiffness in the analysis of frames or beams. If the properties of an element are characterised by two parameters for axial and bending stiffness a similar formulation is still possible using the partition of the stiffness matrix of the element. Similarly we can define the coefficients p_i for the mass and damping matrices.
Minimising the error R with respect to u_{ij}, λ_{ij} and p_i, the following set of equations is obtained:

$$\frac{\partial R}{\partial u_i} = (u - u^*) + K(\omega)\lambda \tag{8a}$$

$$\frac{\partial R}{\partial \omega} = W_1(\omega - \omega^*) + \lambda \frac{\partial K(\omega, p_e)}{\partial \omega} u^T + W_2 \lambda_1 \frac{\partial D(\omega, p_e)}{\partial \omega} \tag{8b}$$

$$\frac{\partial R}{\partial \lambda_i} = K(\omega, p_e)u - F \tag{8c}$$

$$\frac{\partial R}{\partial \lambda_1} = W_2 D(\omega, p_e) \tag{8d}$$

$$\frac{\partial R}{\partial p_i} = \left[\lambda \frac{\partial K(\omega, p_1)}{\partial p_1} u^T + W_2 \lambda_1 \frac{\partial D(\omega, p_1)}{\partial p_1} \ \ldots \ \lambda \frac{\partial K(\omega, p_e)}{\partial p_e} u^T + W_2 \lambda_1 \frac{\partial D(\omega, p_e)}{\partial p_e} \right]^T \tag{8e}$$

3. Numerical solution

The above set of nonlinear equations can be solved by means of any iterative technique suitable for the solution of the nonlinear algebraic equations. By solving the above set of equations, p_i values are obtained, which gives all the parameters of the vibrating structure. In this work the Newton-Raphson method is used to obtain the solutions. A typical problem gives N gradient relations to be zeroed, involving variables $x_i, i = 1,2,...,N$:

$$\frac{\partial F(x_i)}{\partial x_i} = 0 i = 1,2,...,N \tag{9}$$

The vector of partial derivatives appearing in equation (4.11) is the Gradient vector G and the matrix of partial derivatives is the Hessian matrix H:

$$G_i = \frac{\partial F}{\partial x_i} H_{ij} = \frac{\partial^2 F}{\partial x_i \partial x_j}. \tag{10}$$

Solving the above equations, we havey

$$\delta x_j = - [H_{ij}]^{-1} G_i. \tag{11}$$

Next the corrections are added to the solution vector,

$$x_{new} = x_{old} + \delta x_i \tag{12}$$

and the process is iterated to convergence. The problem with local minima can be eliminated if several runs of optimisation routine with different initial values are performed. We can specify the following vectors of the variables:

$$X^T = [u \;\; \omega \;\; \lambda \;\; \lambda_1 \;\; p],$$
$$G^T = \left[\frac{\partial R}{\partial u_i} \;\; \frac{\partial R}{\partial \omega} \;\; \frac{\partial R}{\partial \lambda_i} \;\; \frac{\partial R}{\partial \lambda_1} \;\; \frac{\partial R}{\partial p_i}\right], \tag{13}$$

The Hesian matrix becomes:

$$H = \begin{bmatrix} H_{11} & H_{12} & H_{13} & 0 & H_{15} \\ & H_{22} & H_{23} & H_{24} & H_{25} \\ & & 0 & 0 & H_{35} \\ & & & 0 & H_{45} \\ & & & & H_{55} \end{bmatrix} \tag{14}$$

where,

$$\frac{\partial^2 R}{\partial u_i^2} = H_{11} = I,$$
$$\frac{\partial^2 R}{\partial u_i \partial \omega} = H_{12} = \frac{\partial K(\omega, p_e)}{\partial \omega}\lambda,$$
$$\frac{\partial^2 R}{\partial u_i \partial \lambda_i} = H_{13} = K(\omega, p_e),$$
$$\frac{\partial^2 R}{\partial u_i \partial \lambda_1} = H_{14} = 0,$$
$$\frac{\partial^2 R}{\partial u_i \partial p_i} = H_{15} = \left[\frac{\partial K(\omega, p_e)}{\partial p_1}\lambda \quad \ldots \quad \frac{\partial K(\omega, p_e)}{\partial p_e}\lambda\right].$$
$$\frac{\partial^2 R}{\partial \omega^2} = H_{22} = W_1 + \lambda^T \frac{\partial^2 K(\omega, p_e)}{\partial \omega^2} u + W_2 \lambda_1 \frac{\partial^2 D(\omega, p_e)}{\partial \omega^2}, \tag{15}$$
$$\frac{\partial^2 R}{\partial \omega \partial \lambda_i} = H_{23} = \frac{\partial K(\omega, p_e)}{\partial \omega} u,$$

$$\frac{\partial^2 R}{\partial \omega \partial \lambda_1} = H_{24} = W_2 \frac{\partial D(\omega, p_e)}{\partial \omega},$$

$$\frac{\partial^2 R}{\partial \omega \partial p_i} = H_{25} = \left[\lambda \frac{\partial^2 K(\omega, p_1)}{\partial \omega \partial p_1} u + W_2 \lambda_1 \frac{\partial^2 D(\omega, p_1)}{\partial \omega \partial p_1} \quad \ldots \quad \lambda \frac{\partial^2 K(\omega, p_e)}{\partial \omega \partial p_e} u + \right.$$

$$\left. + W_2 \lambda_1 \frac{\partial^2 D(\omega, p_e)}{\partial \omega \partial p_e} \right],$$

$$\frac{\partial^2 R}{\partial \lambda_i^2} = H_{33} = 0,$$

$$\frac{\partial^2 R}{\partial \lambda_i \partial \lambda_1} = H_{34} = 0,$$

$$\frac{\partial^2 R}{\partial \lambda_i \partial p_i} = H_{35} = \left[\frac{\partial K(\omega, p_1)}{\partial p_1} u \quad \ldots \quad \frac{\partial K(\omega, p_e)}{\partial p_e} u \right],$$

$$\frac{\partial^2 R}{\partial \lambda_1^2} = H_{44} = 0,$$

$$\frac{\partial^2 R}{\partial \lambda_1 \partial p_i} = H_{45} = \left[W_2 \frac{\partial D(\omega, p_1)}{\partial p_1} \quad \ldots \quad W_2 \frac{\partial D(\omega, p_e)}{\partial p_e} \right],$$

$$\frac{\partial^2 R}{\partial p_i^2} = H_{55} = \lambda^T \frac{\partial^2 K(\omega, p_e)}{\partial p_e^2} u + W_2 \lambda_1 \frac{\partial^2 D(\omega, p_e)}{\partial p_e^2}.$$

In the case of a bean structure the dynamic element stiffness matrix (DSM) [27] is given by the formula

$$K_e(\omega) = \frac{p_e}{L^3} \frac{2}{\Delta} \begin{bmatrix} (SCh - CSh)\xi L^2 & SSh\xi^2 L & -(S + Sh)\xi^3 & (Ch - C)\xi^2 L \\ & (SCh - SCh)\xi L^2 & -(Ch - C)\xi^2 L & -(S - Sh)\xi L^2 \\ & & (SCh + CSh)\xi^3 & -SSh\xi^2 L \\ & & & (SCh - CSh)\xi L^2 \end{bmatrix} \tag{16}$$

where $\Delta = 2(1 - CCh)$, $\xi = kL$, $S = Sin\xi$, $C = Cos\xi$, $Sh = Sinh\xi$, $Ch = Cosh\xi$, k is the frequency parameter, usually defined by the boundary conditions. The frequency is related to ξ by means of equation:

$$\omega = \frac{\xi^2}{L^2} \sqrt{\frac{p_e EI}{\rho A}}. \tag{17}$$

It is possible to differentiate analytically the above stiffness matrix and obtain all necessary derivatives in the equations (15).
Using Taylor series expansion, the dynamic stiffness matrix for small ξ can be approximated by the equation:

$$K(\omega) = K - \omega^2 M.$$

where K^e and M^e are given by the following formulae:

$$K^e = \frac{p_e EI}{L^3}\begin{bmatrix} 12 & 6L & -12 & 6L \\ 6L & 4L^2 & -6L & 2L^2 \\ -12 & -6L & 12 & -6L \\ 6L & 2L^2 & -6L & 4L^2 \end{bmatrix}; \; M^e = \frac{\rho AL}{420}\begin{bmatrix} 156 & 22L & 54 & -13L \\ 22L & 4L^2 & 13L & -3L^2 \\ 54 & 13L & 156 & -22L \\ -13L & -3L^2 & -22L & 4L^2 \end{bmatrix}, \tag{18}$$

here M^e is called the consistent mass matrix (CMM).
The lumped element mass matrix (LMM) often used in dynamic finite element analysis is given by the equation

$$M^e = \frac{\rho AL}{2}\begin{bmatrix} 1 & 0 & 0 & 0 \\ 0 & 0 & 0 & 0 \\ 0 & 0 & 1 & 0 \\ 0 & 0 & 0 & 0 \end{bmatrix}.$$

Equations (18) are most often used in finite element analysis. However, we have to note that the expansion on small ξ is equivalent to requirement of small element length L or restricting the analysis to low frequencies.
The derivatives of the determinant can be performed according to the equations provided in below. The calculation of the determinant with respect to the parameters can also be done analytically.

$$\frac{\partial D(\omega)}{\partial \omega} = \begin{vmatrix} -2\omega M_{11} & -2\omega M_{12} & \dots & -2\omega M_{1n} \\ K_{21} - \omega^2 M_{21} & K_{22} - \omega^2 M_{22} & \dots & K_{2n} - \omega^2 M_{2n} \\ \vdots & \vdots & \ddots & \vdots \\ K_{n1} - \omega^2 M_{n1} & K_{n2} - \omega^2 M_{n2} & \dots & K_{nn} - \omega^2 M_{nn} \end{vmatrix} +$$

$$+\begin{vmatrix} K_{11}-\omega^2 M_{11} & K_{12}-\omega^2 M_{12} & \dots & K_{1n}-\omega^2 M_{1n} \\ -2\omega M_{21} & -2\omega M_{22} & \dots & -2\omega M_{2n} \\ \vdots & \vdots & \ddots & \vdots \\ K_{n1}-\omega^2 M_{n1} & K_{n2}-\omega^2 M_{n2} & \dots & K_{nn}-\omega^2 M_{nn} \end{vmatrix} + \dots\dots$$

$$+\begin{vmatrix} K_{11}-\omega^2 M_{11} & K_{12}-\omega^2 M_{12} & \dots & K_{1n}-\omega^2 M_{1n} \\ K_{21}-\omega^2 M_{21} & K_{22}-\omega^2 M_{22} & \dots & K_{2n}-\omega^2 M_{2n} \\ \vdots & \vdots & \ddots & \vdots \\ -2\omega M_{n1} & -2\omega M_{n2} & \dots & -2\omega M_{nn} \end{vmatrix} \tag{19}$$

It is interesting to compare results obtained from the exact dynamic stiffness matrix (DSM), consistent mass matrix (CMM) and lumped mass matrix (LMM). This will be presented in the next part of the paper. Consistent or lump mass matrices are most often used in the technical applications.

4. Numerical results and analysis for a beam structure

Example 1. The loss of bending stiffness due to transverse cracks and corrosion was examined using a ten-element beam model fixed at both ends (Fig. 2). The structure was analysed in two different time periods. In this case, the structure was excited into the first mode and it was necessary to select only two corresponding time periods. Seven elements of the tenelement beam had smaller cross-sectional area than designed, due to corrosion. The loss of cross-sectional areas varied between 0.5% and 3.5% of original values which can be translated to 2% to 13% loss of flexural stiffness. Six elements, some of them already affected by corrosion, had cracks: two on the lower surface, four on the upper surface. The magnitude of stiffness changes varied between 2% and 7%, which can be represented as cracks of a depth from 10% to 30 % of the height of the beam element. The stiffness coefficient for an element affected by corrosion and the crack was simply calculated as multiplication of those two values. This is a correct procedure since the stiffness coefficient for a beam with a transverse crack was calculated in comparison to a beam without a crack. Data for system identification were generated by solving equation (2). A stiffness matrix was assembled in every step of this iterative procedure, to make sure that the data mimic the real behaviour of the structure. In every time-step, curvature of each element was checked and the proper values of stiffness coefficients were assigned. After that, the global stiffness matrix was assembled for the next step. The sample data generated in this way were very smooth, since there was no error of measurement included in the calculation analysis. Displacement can be automatically computed in the case of real measurements of accelerations, displacements can be easily implemented as initial values for the theoretical model in the objective function.

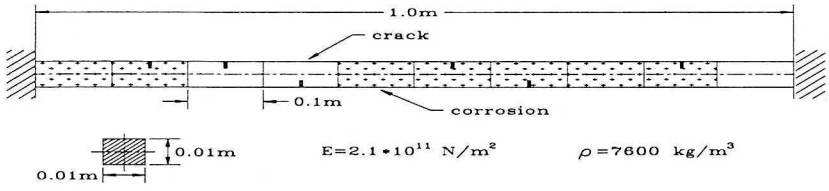

First mode of vibration, configuration # 1

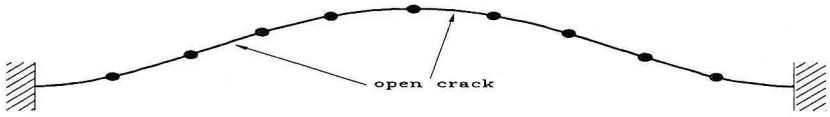

First mode of vibration, configuration # 2

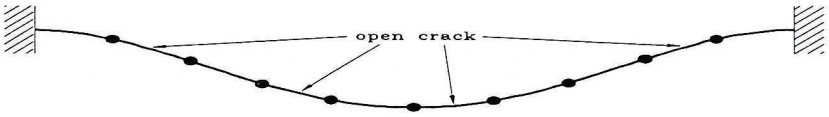

Stiffness	Element No.	1	2	3	4	5	6	7	8	9	10
	Original	1.000	1.000	1.000	1.000	1.000	1.000	1.000	1.000	1.000	1.000
	Corroded element	0.900	0.960			0.970	0.980	0.960	0.940	0.870	
	Cracked element		0.950	0.980	0.900		0.949	0.920		0.970	
	Crack+corrosion		0.912				0.930	0.883		0.844	

Fig. 2

We present below the results obtained from two cases. In the first case the exact dynamic stiffness matrix (DSM) was used. In the second one the static beam stiffness matrix end consistent mass matrix (CMM) was applied. The weights were assumed as $W_1 = 1$. $W_2 = 1$. Initial approximations used for $[\lambda]$ were: $[\lambda] = [1.]$, $[\lambda_1] = [1.]$

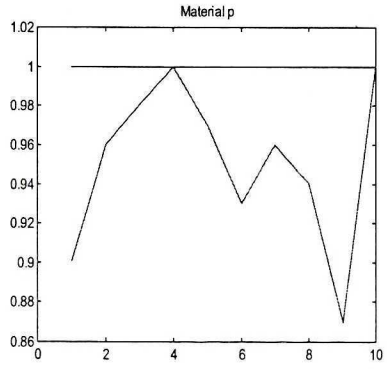

Fig. 3

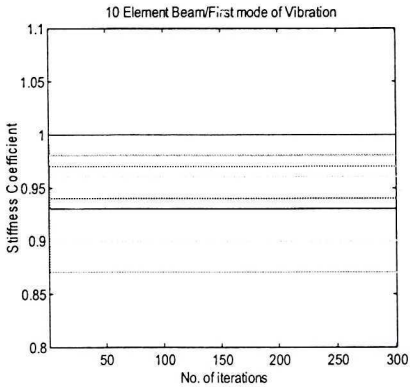

Fig. 4

Fig. 3 presents the initial values of the parameters p_i. Fig. 4 presents the convergence history. We see that correct values of the parameters were obtained after the first iteration.

Table 1. presents the initial values of the stiffness coefficients corresponding to the presence of the cracks and corroded members. We see that the algorithm converged precisely to the original values. The measured value of the frequency was introduced equal to 85.45, the algorithm converged to the value of 79.5 for the first natural frequency.

Table 1.

Identified results from DSM

Element No.	Original Stiffness Coefficient	Identified Stiffness Coefficient
1	0.900	0.90012538861214
2	0.960	0.95998075624026
3	0.980	0.97998077239741
4	1.000	0.99998073695179
5	0.970	0.96998075901856
6	0.930	0.93001925329710
7	0.960	0.96001927474133
8	0.940	0.94001924047432
9	0.870	0.87001927868609
10	1.000	1.00006746348297

Fig. 5. presents the convergence of the error function in the case of DSM algorithm. We can observe smooth and effective convergence of the error to zero.

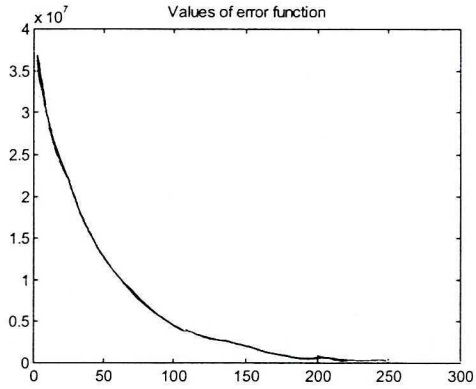

Fig. 5

In the second approach we used the static stiffness matrix of a beam element in consistent mass matrix (CMM). To get the convergence of the solution the following data for the initial approximations were used: for $W_1 = 1e^{-10}$; $W_2 = 1$; Initial $[\lambda]$ approximations were $[\lambda_1] = [1]$; $[\lambda] = [1.0e^{-5}]$. We obtained the results presented in Table 2, the values of the parameters after the convergence. We see that the algorithm converged very precisely to the correct values. However, the value for the natural frequency obtained for the calculations was different than before. The algorithm converged to the value 79.32. The initial value of the natural frequency was 79.56.

Table 2.

Data dentified from CMM

Element No.	Original Stiffness Coefficient	Identified Stiffness Coefficient From DSM
1	0.900	0.90000122148761
2	0.960	0.95999979600018
3	0.980	0.97999979845674
4	1.000	0.99999979520734
5	0.970	0.96999978875268
6	0.930	0.93000016964724
7	0.960	0.96000017705955
8	0.940	0.94000017954965
9	0.870	0.87000017635979
10	1.000	1.00000065042170

Fig. 6 presents the convergence history for CMM algorithm. We see that in this case (Fig. 6) the convergence of the stiffness parameters was reached

very fast. Fig. 7 presents the convergence of the global error increments. Fig 8 depicts the convergence of the global error function. It can be noticed that the error did not converge to zero after 300 iterations.

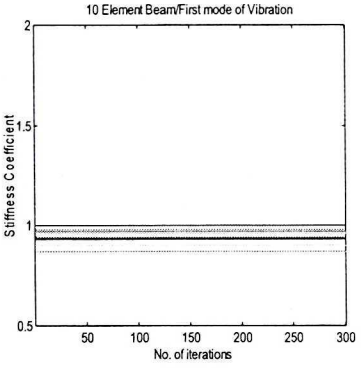

Fig. 6

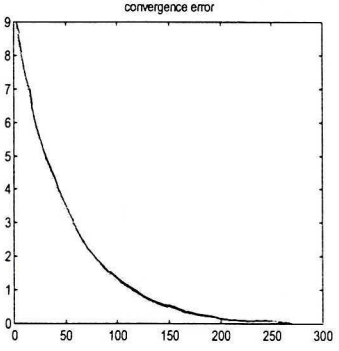

Fig. 7

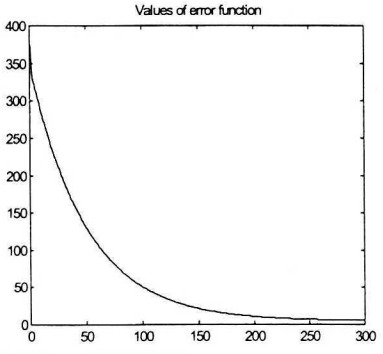

Fig. 8. Values of global error function for LMM

In real life measurement errors must be taken into account. If ordinary accelerometers are used as sensors, the expected error of measurement can be within ±5 to ±20% of the measured value. This error must be included in the

evaluation of the identification procedure since the effectiveness of the method can change dramatically with the uncertainty of the solution. To model of the system with measurement error, data without error was used. Analysis of the influence of the measurement error o n the stability of the system identification revealed that the data with the error taken straight without any smoothing had difficulties in converging.

It should be noticed here that we tested the method on a very simple example of the beam with only 10 elements. In this situation the benefits of the application of dynamic stiffiness matrix is more obvious.

Table 3.

Convergence Frequency and Convergence Error

10^{th} Mode	Initial value	Frequency/Error DSM	Frequency/Error CMM	Frequency/Error LMM
No error	3845.9396	3845.9417/0.0032	3956.7661/0.0742	3845.8372/0.0812
-5% error	3845.9396	3845.9417/0.0032	3845.9525/0.0669	3845.9385/0.0724
-10% error	3845.9396	3845.9417/0.0033	3845.9417/0.0669	
+5% error	3845.9396	3845.9417/0.0031	3845.9536/0.0669	
+10% error	3845.9396	3845.9417/0.0032	3845.9541/0.0669	

Example 2. In the second example a beam fixed at both ends was analysed in two cases. The beam was divided into 20 elements.
The simulated measured data contained the error of 30% introduced to the original natural freequency. The random errors of the nodal displacements data were +-10%. In the second case only nodal displcements were used in identification. The errors of +-10% were introduced to the simulated exact data.
E = 2.1e11 Pa; M = 7830 Kg/M^3, Length of element = 0.10 m; Area of cross-section = 0.0001 m^2; Moment if inertia of the cross-section I_z = 8.30e-10

Case 1: 1^{st} mode of vibration in beam structure.

In this case, 30% error of frequency and ±10% error of displacements were introduced into the initial data. Only displacements (u_y) were used at every node and rotations were not used.

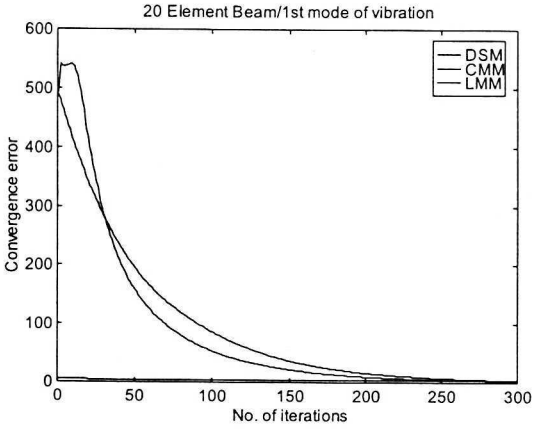

Fig. 9. The figure presents the convergence of the global error for three different algorithms using DSM CSM and LMM

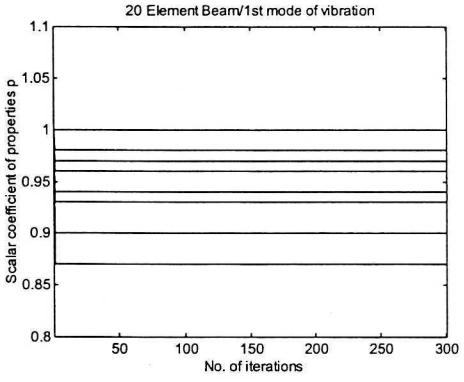

a)

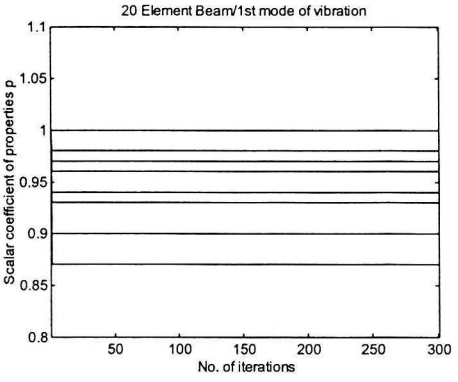

b)

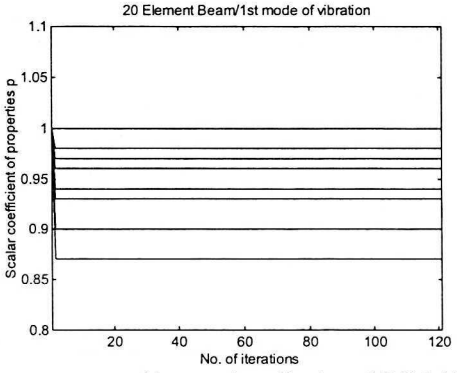

c)

Fig. 10. Presents the convergence history, a) application of DSM, b) CMM, c) LMM

Table 4.

Ist mode of vibration in beam structure

		DSM		CMM		LMM	
No. of element	Original scalar Coefficient Parameter	Identified scalar Coefficient Parameter	Error %	Identified scalar Coefficient Parameter	Error %	Identified scalar Coefficient Parameter	Error %
1	0.9000	0.9000		0.9000		0.9000	
2	0.9000	0.9000		0.9000		0.9000	
3	0.9600	0.9600		0.9600		0.9600	
4	0.9600	0.9600		0.9600		0.9600	
5	0.9800	0.9800		0.9800		0.9800	
6	0.9800	0.9800		0.9800		0.9800	
7	1.0000	1.0000		1.0000		1.0000	
8	1.0000	1.0000		1.0000		1.0000	
9	0.9700	0.9700		0.9700		0.9700	
10	0.9700	0.9700		0.9700		0.9700	
11	0.9300	0.9300		0.9300		0.9300	
12	0.9300	0.9300		0.9300		0.9300	
13	0.9600	0.9600		0.9600		0.9600	
14	0.9600	0.9600		0.9600		0.9600	
15	0.9400	0.9400		0.9400		0.9400	
16	0.9400	0.9400		0.9400		0.9400	
17	0.8700	0.8700		0.8700		0.8700	
18	0.8700	0.8700		0.8700		0.8700	
19	1.0000	1.0000		1.0000		1.0000	
20	1.0000	1.0000		1.0000		1.0000	
Frequency	82.08	82.9621	0.67	83.9591	2.26	96.4341	17.49
Convergence error		0.67		1.38		1.79	

Case 2: 10th mode of vibration in beam structure

In this case, 30% error of frequency and ±10% random error of displacements using were introduced. Displacements (u_y) at every next node were used and rotations were not used.

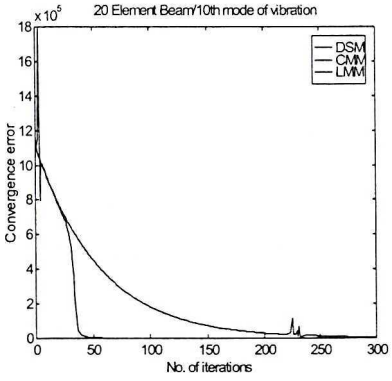

Fig. 11. Convergence history for global error

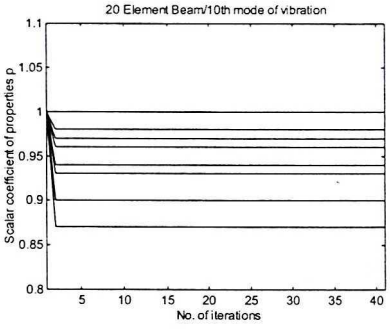

a)

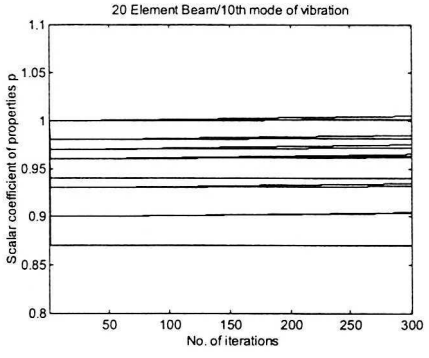

b)

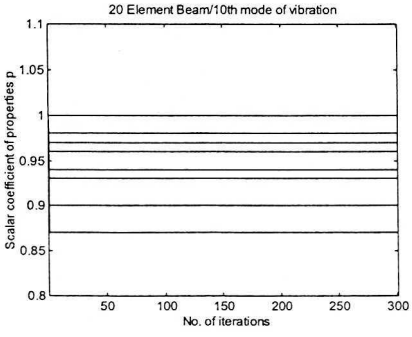

c)

Fig. 12. Convergence history for stiffness parameters and different algorithms
a) DMM, b) CCM, c) LMM

Table 5.

10^{th} mode of vibration in beam structure

		DSM		CMM		LMM	
No. of element	Original scalar Coefficient Parameter	Identified scalar Coefficient Parameter	Error %	Identified scalar Coefficient Parameter	Error %	Identified scalar Coefficient Parameter	Error %
1	0.9000	0.9000	0	0.9000	0	0.9038	0.42
2	0.9000	0.9000	0	0.9000	0	0.9045	0.50
3	0.9600	0.9600	0	0.9600	0	0.9617	0.18
4	0.9600	0.9600	0	0.9600	0	0.9650	0.52
5	0.9800	0.9800	0	0.9800	0	0.9816	0.16
6	0.9800	0.9800	0	0.9800	0	0.9849	0.50
7	1.0000	1.0000	0	1.0000	0	1.0016	0.16
8	1.0000	1.0000	0	1.0000	0	1.0048	0.18
9	0.9700	0.9700	0	0.9700	0	0.9717	0.18
10	0.9700	0.9700	0	0.9700	0	0.9750	0.52
11	0.9300	0.9300	0	0.9300	0	0.9318	0.19
12	0.9300	0.9300	0	0.9300	0	0.9346	0.49
13	0.9600	0.9600	0	0.9600	0	0.9629	0.30
14	0.9600	0.9600	0	0.9600	0	0.9630	0.31
15	0.9400	0.9400	0	0.9400	0	0.9403	0.03
16	0.9400	0.9400	0	0.9400	0	0.9401	0.01
17	0.8700	0.8700	0	0.8700	0	0.8704	0.05
18	0.8700	0.8700	0	0.8700	0	0.8701	0.01
19	1.0000	1.0000	0	1.0000	0	1.0003	0.03
20	1.0000	1.0000	0	1.0000	0	1.0003	0.03
Frequency	3845.9397	3850.5133	0.12	4922.6193	27.97	4165.0085	8.30
Convergence error		11.43		70.74		4.20	

Example 3. The frame presented in Fig. 9 was analysed in two cases. In the first mode of vibrations and in the 10th mode.

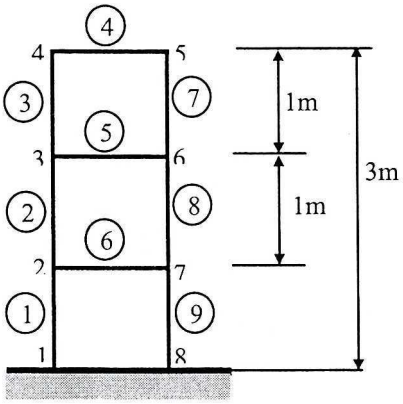

Fig. 13. 9 elements frame

Case 1: 1st mode of vibration of frame structure.

In this case, 30% error of frequency and ±10% random error of displacements were introduced using the random function. Displacements (u_x and u_y) at every next node were used and rotations were not used.

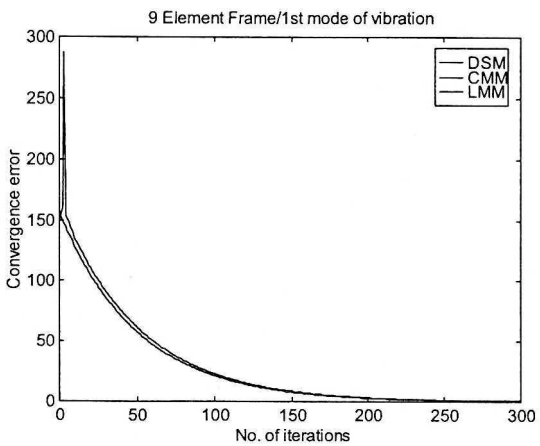

Fig. 14. Comparison of the convergence error for three algorithms

The results of the identification are presented in Table 6.

Case 2: 10th mode of vibration in frame structure. In this case, 30% error of frequency and ±10% error of displacements were introduced. Displacements (u_x and u_y) at every next node were used and rotations were not used.

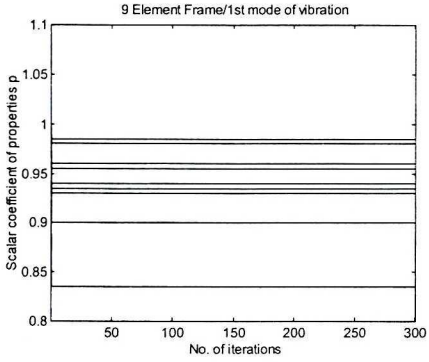

a)

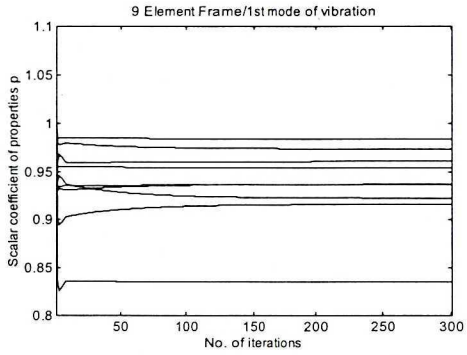

b)

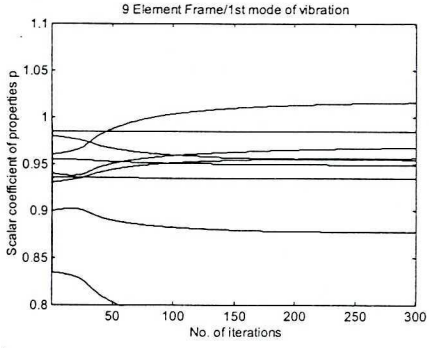

c)

Fig. 15. The history of the convergence of the stiffness coefficients for different algorithms. a) DSM, b) CSM and c) LMM

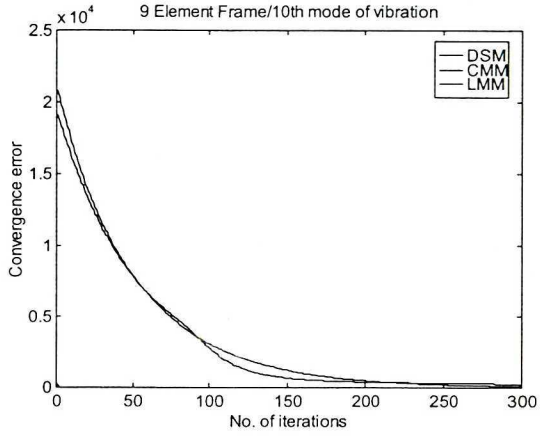

Fig. 16. Comparison of the convergence error for different algorithms

Table 6.

Ist mode of vibrations of frame structure

		DSM		CMM		LMM	
No. of element	Original scalar Coefficient Parameter	Identified scalar Coefficient Parameter	Error %	Identified scalar Coefficient Parameter	Error %	Identified scalar Coefficient Parameter	Error %
1	0.9000	0.9000	0.00	0.9161	1.79	0.8776	-2.49
2	0.9600	0.9600	0.00	0.9606	0.06	1.0152	5.75
3	0.9800	0.9799	-0.01	0.9735	-0.66	0.9543	-2.62
4	0.9850	0.9849	-0.01	0.9841	-0.09	0.9849	-0.01
5	0.9350	0.9350	0.00	0.9363	0.14	0.9346	-0.04
6	0.9550	0.9549	-0.01	0.9540	-0.10	0.9489	-0.64
7	0.9300	0.9299	-0.01	0.9369	0.74	0.9562	2.82
8	0.8350	0.8350	0.00	0.8349	-0.01	0.7703	-7.75
9	0.9400	0.9400	0.00	0.9226	1.85	0.9672	2.89
Frequency	13.04	13.1490	1.23	16.6869	27.22	13.9459	6.95
Convergence error		0.19		0.66		0.85	

Table 7.

Results for the 10^{th} mode of vibration of the frame structure. We see the big error of the frequency from CMM and LMM

		DSM		CMM		LMM	
No. of element	Original scalar Coefficient Parameter	Identified scalar Coefficient Parameter	Error %	Identified scalar Coefficient Parameter	Error %	Identified scalar Coefficient Parameter	Error %
1	0.9000	0.8999	-0.01	1.0296	Cras-hed	0.9157	1.74
2	0.9600	0.9596	-0.04	1.0856		0.9623	0.24
3	0.9800	0.9798	-0.02	1.1528		0.9728	-0.73
4	0.9850	0.9851	0.01	1.1135		0.9846	-0.04
5	0.9350	0.9351	0.01	1.0620		0.9358	0.08
6	0.9550	0.9550	0.00	1.0931		0.9544	-0.06
7	0.9300	0.9299	-0.01	1.1002		0.9378	0.84
8	0.8350	0.8345	-0.06	0.9734		0.8328	-0.26
9	0.9400	0.9398	-0.02	1.1371		0.9227	-1.84
Frequency	503.60	504.0761	0.09	631.1444	25.4	645.1248	28.10
Convergence error		1.681		15.38		8.79	

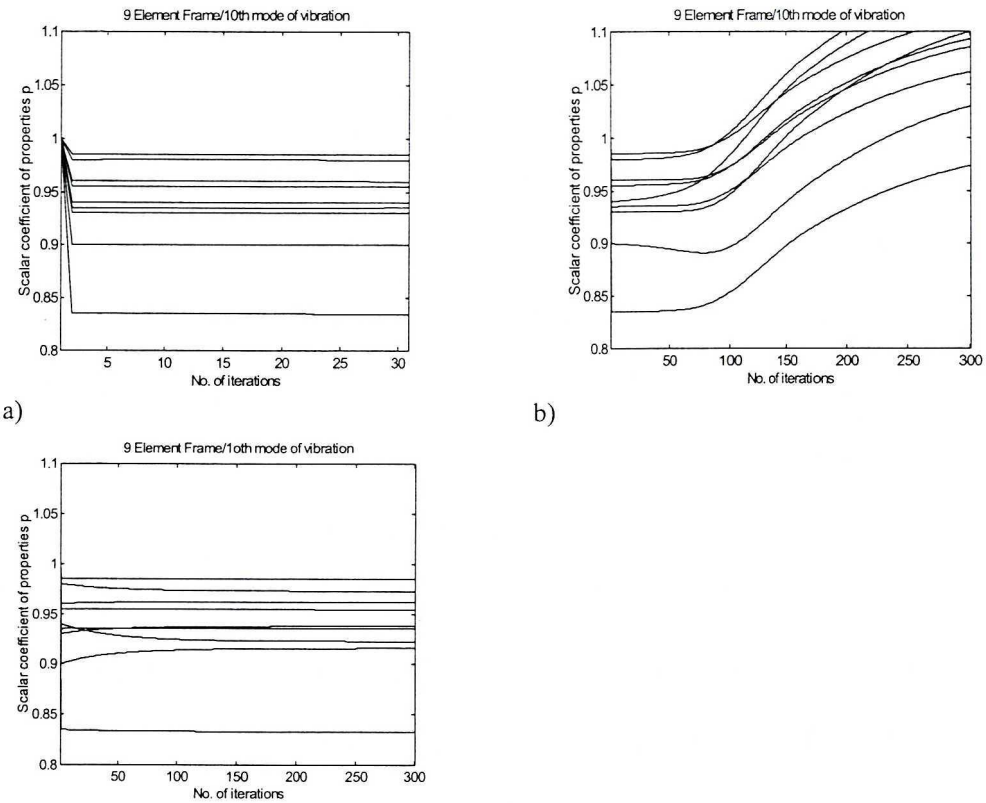

Fig. 17. Comparison of the convergence history for the stiffness parameters.
a) DSM, b) CMM, c) LMM

9. Conclusions

We observe that both application of the dynamic stiffness matrix (DSM) and the consistent mass matrix (CMM) generated correct results as regards the stiffness parameters. Using the first mode of the vibrations in the identification process we did not observe the significant difference in the results of the identification. The parameters p were calculated with very high precision in both cases. The error was less then 0.01%, which is a much better result that reported in the previous paper [26], [37]. This result was obtained by inclusion of the natural frequencies into identification process and assumption of the harmonic motion. However, for the tenth mode of the vibrations the differences are much larger. For example in one case, the algorithm based on the consistent mass matrix (CMM) did not converge when the DSM gave good convergence. We observed in general the superior behaviour of the approach based on DSM. The convergence of the results was

cImuch faster, stable and better in the case of incorrect initial data. The values of the natural frequencies obtained from the iteration process using dynamic stiffness matrix were much more accurate than using consistent mass matrix or lump mass matrix.

Manuscript received by Editorial Board, January 22, 2004;
final version, June 28, 2004.

REFERENCES

[1] Adams R. D., Cawley P.: "The Location of Defects in Structures from Measurement of Natural Frequencies", *Journal of Strain Analysis*, Vol. 14, 1979, pp. 49÷57.

[2] Baruh H., Ratan S.: "Damage Detection in Flexible Structures", *Procedings of the Eighth VPI & SU Symposium on Dynamic and Control of Large Structures* (Blacksburg, VA), edited by L. Meiroritch, 1991, pp. 171÷179.

[3] Christides S., Barr A. D. S.: "One Dimensional Theory of Cracked Bernoulli-Euler Beams", *Internatioal Journal of Mechanical Sciences*, Vol. 26 (11÷12), 1984, pp. 639÷648.

[4] Cuiping L., Smith S. W.: "Hybrid Approach for Damage Detection in Flexible Structures", *Journal of Guidance, Control and Dynamics*, Vol. 18, 1995, pp. 419÷425.

[5] Flanigan C.: "Correction of Finite Element Models Using Mode Shape Design Sensitivity", *Proceedings of the Ninth International Modal Analysis Conference, Society for Experimental Mechanics*, Bethel, CT, 1991, pp. 84÷88.

[6] Friswell M., Mottershead I.: "Finite element Updating in Structural Dynamics", Kluver Academic Publishers.

[7] Goodwin C. G., Payne R. A.: "Dynamic System Identification, Experiments, Design and Data Analysis", *Academic Press*, New York, 1977.

[8] Hajela P., Soeiro F. J.: "Structural Damage Detection Based on Static and Modal Analysis", *AIAA Journal*, Vol. 28, No. 1, 1990, pp. 1110÷1115.

[9] Hasan W. M.: "Crack Detection from the variation of the Eigenfrequencies of a Beam on Elastic Foundation", *Engineering Fracture Mechanics*, Vol. 52(3), 1995, pp. 409÷421.

[10] Hendricks S. L., Hayes S. M., Junkins J. L.: "Structural Parameter Identification for Flexible Spacecraft", *Proceedings of the AIAA 22nd Aerospace Science Meeting* (Reno, NV), AIAA, New York, 1984.

[11] Hetenyi M.: "Deflection of Beams of Varying Cross Section", *Journal of Applied Mechanics, Trans. ASME*, Vol. 59, pp. A49÷A52, 1937.

[12] Ibrahim S. R., Mikulcik E. C.: "A method for the Direct Identification of Vibration Parameters from the Free Response", *The Shock and Vibration Bulletin*, Vol. 47 (4), 1977, pp. 183÷198.

[13] Jelonnek B., Kammeyer K.-D.: "Improved Methods for the Blind System Identification Using Higher order Statistics", *IEEE Transactions on Signal Processing*, Vol. 40, 1992, pp. 2947÷2960.

[14] Juang J.-N.: "An Overview of Recent Advances in Systems Identification", *A Collection of Technical Papers: 34th AIAA/ASME/ASCE/AHS/ASC Structures, Structural Dynamic, and Materials Conference* (La Jolla, CA), 1993, pp. 3342÷3352.

[15] Kabe A. M.: "Stiffness Matrix Adjustment Using Mode Data", *AIAA Journal*, Vol. 23, No. 9, 1985, pp. 1431÷1436.

[16] Kirmser P. G.: "The Effect of Discontinuities on the Natural Frequency of Beams", *Proceedings of the ASTM*, Vol. 44, 1944, pp. 897.

[17] Lin R. M.: "Analytical Model Improvement Using Modified IEM", *Proceedings of the International Conference on Structural Dynamics Modeling, National Agency for Finite Element Methods and Standards*, Glasgow, Scotland, UK, 1993, pp. 181÷194.

[18] Lindholm B. E., West R. L.: "System Identification of Finite Element Modeling Parameters Using Experimental Spatial Dynamic Modeling", *First International Conference on Vibration Measurements by Laser Techniques* (Ancona, Italy), 1994, pp. 450÷462.

[19] Lukasiewicz S. A., Stanuszek M.: "Constrained, Weighted, Least Square Technique for Correcting Experimental Data", *Proceedings of the Conference "Computational Methods and Experimental Mechanics VI"* Elsevier Applied Science, 1993.

[20] Lukasiewicz S. A., Babaei R.: "On Identification of Dynamic Systems", Computational Methods and Experimental Measurement VII, *Computational Mechanics Publications*, Southampton, Boston Editors G. M. Carlomagno, C. A. Brebia, 1995.

[21] Lukasiewicz, S. A. and Babaei, R., "Effects of Dependent Variables and Instrumental Errors in Filtering of the Experimental Data", *Communications in Numerical Methods in Engineering*, Vol. 12, 1996.

[22] McGowan, P. E., Smith, S. W., Javeed, M., "Experiments for Locating Damaged Members in a Truss Structure", *Proceedings of the Second USAF/NASA Workshop on System Identification and Health Monitoring of Precision Space Structures*, Vol. 2, Pasadena, Ca, March, 1990, pp. 571÷615.

[23] Morassi A., "Crack-Induced Changes in Eigenparameters of Beam Structures", *Journal of Engineering Mechanics*, ASCE, Vol. 119, 1993, pp. 1798÷1803.

[24] Ostachowicz W. M., Krawczuk M.: "Analysis of the Effect of Cracks on the Natural Frequencies of a Cantilever Beam", *Journal of Sound and Vibration*, Vol. 150 (2), 1991, pp. 191÷201.

[25] Pabst U., Hagedom, P.: "On the Identification of Localized Losses of Stiffness in Structures", *Structural Dynamics of Large Scale and Complex Systems – ASME 1993*, DE-Vol. 59, 1993, pp. 99÷104.

[26] Palka K.: "Detection of Cracks and Corroded Members in Structures from Dynamic Responses, Thesis (M.Sc.), University of Calgary, 1996.

[27] Doyle J. F.: "Static and Dynamic Analysis of Structures with an Emphasis on Mechanics and Computer Matrix Methods", *Kluver Academic Publishers*. Dordrecht, Boston, London.

[28] Petroski H. J.: "Simple Static and Dynamic Models for the Cracked Elastic Beam", *International Journal of Fracture*, Vol. 17, 1981, pp. R71÷R76.

[29] Qian G.-L., Gu S.-N., Jiang J.-S.: "The Dynamic Behaviour and Crack Detection of a Beam with Crack", *Journal of Sound and Vibration*, Vol. 138(2), 1990, pp. 233÷243.

[30] Ricles J. M., Kosmatka J. B.: "Damage Detection in Elastic Structures Using Vibratory Residual Forces and Weighted Sensitivity", *AIAA Journal*, Vol. 30, No. 9, 1992, pp. 2310÷2316.

[31] Rizos P. F., Aspragathos N., Dimarogonas A.D.: "Identification of Crack Location and Magnitude in Canilever Beam from the Vibration Modes", *Journal of Sound and Vibration*, Vol. 138(3), 1990, pp. 381÷388.

[32] Smith S. W., Hendricks S. L.: "Damage Detection and Location in Space Trusses", *AIAA SDM Issues of the International Space Station: A Collection of Technical Papers*, Williamsburg, VA, AIAA, Washington DC, 1988, pp. 56÷63.

[33] Smith S. W., Beattie C. A.: "Simultaneous Expansion and Orthogonalization of Measured Modes for Structure Identification", *AIAA Dynamics Specialistic Conference: A Collection of Technical Papers*, Long Beach, Ca), AIAA, Washington DC, 1990, pp. 261÷270.

[34] Thomson W. T.: "Vibration of Slender Bars With Discontinuities in Stiffness", *Journal of Applied Mechanics*, Vol. 16, 1949, pp. 203÷207.

[35] Yuen M. M. F.: "A Numerical Study of the Eigenparameters of a Damaged Cantilever", *Journal of Sound and Vibration*, Vol. 103(3), 1985, pp. 301÷310.
[36] Zehn M., Wahl F., Schmidt G.: "Verification and Adjustment of Dynamic Structural Finite Element Models by Experimental Model Analysis Data", *Computational Methods and Experimental Measurements VII. Computational Mechanics Publications*, Southampton, Boston, Editors G. M. Carlomagno, C. A. Brebia.
[37] Lukasiewicz S. A., Palka K.: "Least square method for detection of defects in structures from dynamic responses". *The Archive of Mechanical Enginnering*, Vol. XLIV, 1997, pp. 226÷263.
[38] Richards T. H., Leung Y. T.: "An accurate method in structural vibration structures analysis", *Journal of Sound and Vibration*, 55(3), 1977, pp. 363÷376.
[39] Gaboussi W. J., Garret J. H.: "Use of Neural Network in Detection of Structural Damage". *Computers and Structures*, Vol. 42, No. 4, 1992, pp. 649÷659.

Zastosowanie dynamicznej macierzy sztywności do identyfikacji pęknięć w belkach i ramach

Streszczenie

W artykule przedyskutowano problem dokładności wibracyjnych technik identyfikacji, stosowanych przy wykrywaniu pęknięć i skorodowanych członów konstrukcji belkowych i ramowych. Obecność pęknięć zmęczeniowych powoduje zwykle bardzo małe zmiany sztywności elementów belkowych konstrukcji. W celu wykrycia tych zmian niezbędne jest zastosowanie najbardziej precyzyjnych metod matematycznych. W procedurze identyfikacji, opartej na metodzie najmniejszych kwadratów, stosuje się modele elementów skończonych (FEM) danej konstrukcji, a jako źródło informacji wykorzystuje się zmierzoną odpowiedź dynamiczną i częstotliwości drgań własnych. Zastosowanie Dynamicznej Macierzy Sztywności (DSM) [1] do reprezentacji wszystkich więzów i równań modalnych pozwala na przedstawienie procesu identyfikacji w bardzo dokładnej i efektywnej formie matematycznej. Metoda detekcji zmian strukturalnych, użyta w przedstawionej pracy, była opisana w poprzedniej publikacji autorów [2]. W algorytmach identyfikacji bardzo często używa się Macierzy Zgodnych Mas (CMM) i Macierzy Mas Skupionych (LMM). Jak wykazano, zastosowanie podejścia uproszczonego (CMM i LMM), może prowadzić do małej dokładności i słabej zbieżności algorytmów identyfikacji. Niemniej, zastosowanie macierzy mas typu CMM nie wprowadza istotnych błędów. Algorytmy były testowane na symulowanych danych numerycznych dla dziesięcioelementowych ram belkowych.